AN ACCURATE AND EFFICIENT DESIGN TOOL FOR LARGE CONTOURED BEAM REFLECTARRAYS

Min Zhou[1,2], Stig B. Sørensen[1], Erik Jørgensen[1], Peter Meincke[1], Oleksiy S. Kim[2], Olav Breinbjerg[2], and Giovanni Toso[3]

[1]*TICRA, DK-1201 Copenhagen, Denmark*
[2]*Department of Electrical Engineering, Technical University of Denmark, DK-2800 Kgs. Lyngby, Denmark*
[3]*ESA-ESTEC, 2200 AG Noordwijk, The Netherlands*

ABSTRACT

An accurate and efficient tool for the design of contoured beam reflectarrays is presented. It is based on the Spectral Domain Method of Moments, the Local Periodicity approach, and a minimax optimization algorithm. Contrary to the conventional phase-only optimization techniques, the geometrical parameters of the array elements are directly optimized to fulfill the far-field requirements. The design tool can be used to optimize reflectarrays based on a regular grid as well as an irregular grid. Both co- and cross-polar radiation can be optimized for multiple frequencies, polarizations, and feed illuminations. Two offset contoured beam reflectarrays that radiate a high-gain beam on an European coverage have been designed, manufactured, and measured at the DTU-ESA Spherical Near-Field Antenna Test Facility. An excellent agreement is obtained for the simulated and measured patterns. To show the design tool's ability to optimize electrically large reflectarrays, a 50×50 square wavelengths contoured beam reflectarray has been designed.

Key words: Printed reflectarrays, accurate antenna analysis, method of moments (MoM), measurements, contoured beam, optimization, satellite antennas.

1. INTRODUCTION

Printed reflectarrays provide a way for realizing low-cost, high-gain antennas for space applications and are the subject of increasing research interest [1–3]. For satellite broadcasting and telecommunication applications, the most often used antenna is the shaped reflector antenna. Although the shaped reflector antenna is a mature technology, both in terms of manufacturing and simulation tools, they suffer from large volume and mass, as well as high cost of manufacturing. Printed reflectarrays on the other hand consist of a flat surface, they are light, easy and cheap to manufacture, and can be packed more compactly, saving volume for the launch.

To obtain a certain antenna performance, several degrees of freedom in printed reflectarrays can be utilized, e.g. the size [4], the shape [5–7], the orientation [8], and the position [9, 10] of the array elements, as well as the shape of the reflecting surface [11] of the reflectarray. An accurate and efficient design procedure that is capable of including all these parameters is a challenging task.

The conventional approach for the design of contoured beam reflectarrays is using a phase-only optimization technique (POT) [12, 13]. Initially, a phase-only synthesis is performed to determine the phase distribution on the reflectarray surface. The array elements are subsequently optimized, element by element, to match the required phase distribution. Several contoured beam reflectarrays have been designed using this technique [13–15].

Although the POT is efficient, since the analysis of all array elements at each iteration is avoided, a direct optimization technique, where all the array elements are simultaneously optimized, may produce more optimal designs. Such approaches are presented in [16, 17]. In [16], a small contoured beam reflectarray was designed and measured. However, significant discrepancies between simulations and measurements were observed, and it was concluded that further work is needed to improve the accuracy of the analysis. In [17], a direct optimization technique where also the position of the array elements can be included in the optimization is presented. The array elements are located in a strongly distorted grid and a full-wave Method of Moments (MoM) is used in the optimization. This involves a high computational burden.

In this work, we present a new direct optimization technique, which is both efficient and accurate. It is based on the Spectral Domain Method of Moments (SDMoM) assuming Local Periodicity (LP) and a minimax optimization algorithm. The direct optimization technique can be used for the design of reflectarrays based on a regular grid as well as for reflectarrays based on an irregular grid. To verify the accuracy of the direct optimization technique, two offset contoured beam reflectarrays that radiate a high-gain beam on an European coverage have been designed, manufactured, and measured at the DTU-ESA Spherical Near-Field Antenna Test Facility [18]. An excellent agreement is obtained between simulations and measurements, thus validating the direct

optimization technique and the LP approach.

Some of the results presented in this paper have been published elsewhere [19, 20], but are included to give a complete overview of the direct optimization technique.

This paper is organized as follows. Section 2 describes the direct optimization technique. The reflectarray samples are described in Section 3 where also the simulations are compared to the measured data. In Section 4, the design of a 50×50 square wavelengths contoured beam reflectarray is presented, and conclusions and on-going work are given in Section 5.

2. DIRECT OPTIMIZATION TECHNIQUE

The direct optimization technique (DOT) is based on a gradient-based method for non-linear minimax optimization.

The far-field requirements are specified in a number of far-field stations in the u-v plane where $u = \sin\theta\cos\phi$ and $v = \sin\theta\sin\phi$. At each iteration, the maximum difference between realized and specified objectives are minimized. The optimization variables are the geometrical parameters of the array elements, e.g. the size and position of the array element. Both co- and cross-polar radiation can be optimized for multiple frequencies, polarizations, and feed illuminations.

To calculate the far-field during the optimization, the Floquet harmonics technique [21, Technique II] is used. It is based on the field equivalence principle and uses the scattering matrices determined from the fundamental Floquet harmonics through the SDMoM formulation. To evaluate the final optimized reflectarray, the more accurate continuous spectrum technique [21, Technique III] is used.

To ensure an accurate and yet efficient calculation of the scattering matrices, higher-order hierarchical Legendre basis functions as described in [22] are used to represent the electric currents on the array elements. These basis functions can be applied to any arbitrarily shaped array elements, and have been demonstrated to yield very accurate results [23]. The versatility of the higher-order hierarchical Legendre basis functions is an important feature in the DOT as it enables the optimization of reflectarrays consisting of non-canonical element shapes, e.g. those reported in [5–7].

To utilize the position of the array elements in the DOT, an irregular distribution of element positions is obtained through a mapping from a regular to an irregular grid. Constraints on the mapping must be enforced to ensure the area of the reflectarray surface is efficiently utilized. In [17], the edges of the reflectarray are not constrained. In our case, the edges are kept fixed to avoid any undesired increase in the antenna size.

The mapping used in this work is acquired by adding a distortion to the regular grid. Let us define (α, β) as normalized coordinates in the regular grid such $|\alpha| \leq 1$ and $|\beta| \leq 1$. The new normalized coordinates in the irregular grid is then given by $(\alpha', \beta') = (\alpha + f_x, \beta + f_y)$, where

$$f_x(\alpha,\beta) = (\alpha-1)(\alpha+1)\sum_{p=0}^{\mathrm{P}}\sum_{q=0}^{\mathrm{Q}} c_{pq}T_p(\alpha)T_q(\beta), \tag{1a}$$

$$f_y(\alpha,\beta) = (\beta-1)(\beta+1)\sum_{p=0}^{\mathrm{P}}\sum_{q=0}^{\mathrm{Q}} d_{pq}T_p(\alpha)T_q(\beta). \tag{1b}$$

Herein, T_i is the Chebyshev polynomial of order i, and c_{pq} and d_{pq} are the distortion coefficients. The factors in front of the summations are boundary conditions that ensure the edges of the reflectarray are kept fixed.

The degree of the distortion is governed by the values of c_{pq} and d_{pq} and the order i. To avoid strong distortions, where array elements overlap, bounds are specified for the values of c_{pq} and d_{pq}, and the maximum order of the Chebyshev polynomials should not exceed 4. To achieve strong irregularities, only 2-6 distortion coefficients are needed [19]. The distortion coefficients c_{pq} and d_{pq} are included as optimization variables to optimize the positions of the array elements.

Due to the grid distortion, the array elements are now positioned in a non-periodic lattice and the LP approach can no longer be applied. Therefore, a new unit-cell must be defined to approximate locally these non-periodic cells. Lets us define the center of the distorted cell as the intersection of the two diagonal lines of the distorted cell. The array element is rotated to orient in parallel of the bisector lines of the two diagonal lines of the distorted cell, and located at the center of the distorted cell. This is illustrated in Fig. 1a, where the diagonal and bisector lines are shown as the solid and dashed lines, respectively. Now, we define an equivalent square cell with the same area as the distorted cell. The equivalent cell has the same center as the distorted cell and is oriented parallel to the bisector lines in the distorted cell. This is shown in Fig. 1b. The equivalent cell is used in the LP computations to calculate the scattering matrices. It was shown in [19] that the accuracy of the LP approach for the analysis reflectarrays with irregularly positioned array elements is very good, even for the cross-polar radiation. Consequently, the LP approach can be used to analyze and optimize reflectarrays with regularly positioned as well as irregularly positioned array elements.

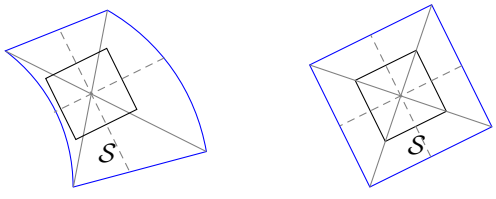

(a) (b)

Figure 1. An example of (a) a distorted cell and (b) its equivalent square cell.

To circumvent the calculation of the scattering matrices of all array elements at each optimization iteration, the scattering matrices are calculated in advance and stored in a look-up table, which is accessed during the optimization. For a given frequency and substrate, the scattering matrices depend on: illumination angles, geometry of the array element, and unit-cell dimensions. For the reflectarrays presented in this paper, we have found that a sufficient accuracy can be obtained by using approximately $N_{\mathrm{el}} = 60$ patch samples, $N_{\mathrm{inc}} = 60$ incident angles, and $N_{\mathrm{cell}} = 50$ different unit-cell sizes, yielding a total of $N_{\mathrm{total}} = N_{\mathrm{el}} N_{\mathrm{inc}} N_{\mathrm{cell}} = 60 \cdot 60 \cdot 50 = 180000$ scattering matrix calculations per frequency. The computation time on a standard laptop computer is approximately one hour. The look-up table can be reused and needs only to be recalculated if another substrate or frequency is used.

For large reflectarrays, where the number of array elements exceeds 10000, the number of optimization variables becomes prohibitively large and the computational burden of the optimization is too high to be run on a standard laptop computer. Thus, to reduce the number of optimization variables, cubic splines have been included in the DOT to represent the sizes of the array elements

$$s(x,y) = \sum_{i}^{I} \sum_{j}^{J} b_{ij} B_i(x) B_j(y). \qquad (2)$$

Herein, $s(x,y)$ describes the sizes of the array elements at coordinates (x,y), b_{ij} are the spline coefficients, and $B_i(x)$ and $B_j(y)$ are the cubic splines. The spline coefficients b_{ij} are the optimization variables used to optimize the sizes of the array elements. However, the variation of the dimensions of the array element over the reflectarray surface can have discontinuities when the scattered phase is required to jump after a complete 360° cycle. Such discontinuities are hard to represent using splines. As a result, a design obtained using splines is inferior compared to a design where the array elements are directly optimized (unless the number of splines and array elements are equal). It is expected the spline representation can be improved if a periodic mapping between $s(x,y)$ and the sizes of the array elements is used such the discontinuities can be taken into account. This is subject to on-going work. Nevertheless, the current spline implementation can be used to generate a design, which can be used as a starting point for the more rigorous optimization where the array elements are directly optimized. In this way, the number of optimization iterations, and hence the overall computation time, that is needed for the rigorous optimization, can be reduced.

For more details on the analysis methods and the look-up table used in the DOT, the reader is referred to [21, 23–25].

3. VALIDATION BY MEASUREMENTS

To validate the DOT, two offset contoured beam reflectarrays that radiate a high-gain beam on an European coverage with cross-polar suppression within the same coverage and sidelobe suppression within a southern African contour have been designed, manufactured, and measured at the DTU-ESA Spherical Near-Field Antenna Test Facility, see Figure 2. The coverages seen from the longitude 0° geostationary orbital position are shown in Figure 3. The reflectarray parameters are summarized in Table 1 with respect to the coordinate system depicted in Figure 4.

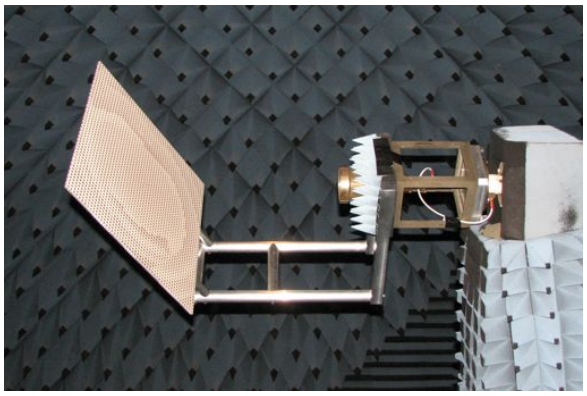

Figure 2. Sample I in the DTU-ESA Spherical Near-Field Antenna Test Facility.

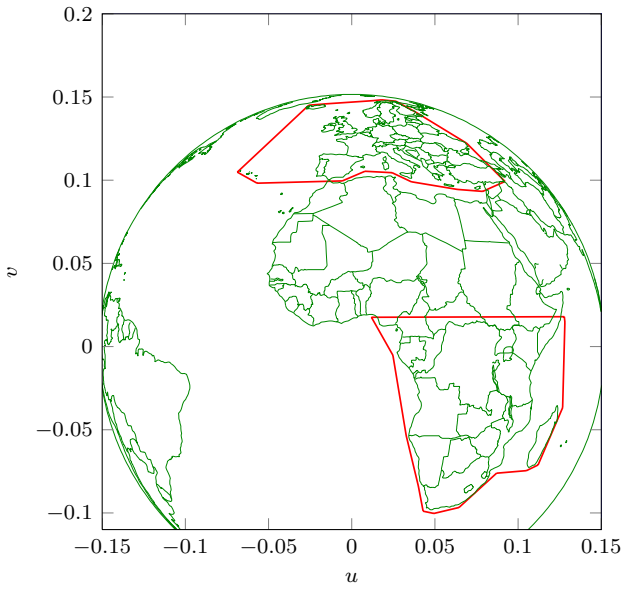

Figure 3. European and southern African coverages seen from the longitude 0° geostationary orbital position.

3.1. Reflectarray Samples

The mask layout of the two reflectarray samples are shown in Figure 5.

The reflectarray in Figure 5a, sample I, is a regular reflectarray where the array elements are positioned in a regular grid. It is optimized for two orthogonal linear

Table 1. Reflectarray Sample Data

Frequency	$10\,\mathrm{GHz}$
Reflectarray dimension	$600\,\mathrm{mm} \times 600\,\mathrm{mm}$
Number of elements	50×50
Relative permittivity	$\epsilon_\mathrm{r} = 3.66$
Loss tangent	$\tan\delta = 0.0037$
Substrate thickness	$h = 0.762\,\mathrm{mm}$
Feed distance	$d_\mathrm{f} = 0.6\,\mathrm{m}$
Feed offset angle	$\theta^\mathrm{i} = 30^\circ$, $\phi^\mathrm{i} = 0^\circ$
Main coverage	European coverage
Cross-polar suppression	European coverage
Sidelobe suppression	Southern African coverage

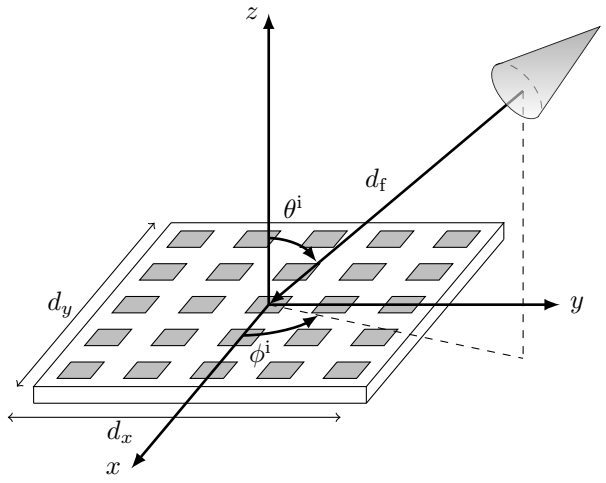

Figure 4. Reflectarray geometrical parameters.

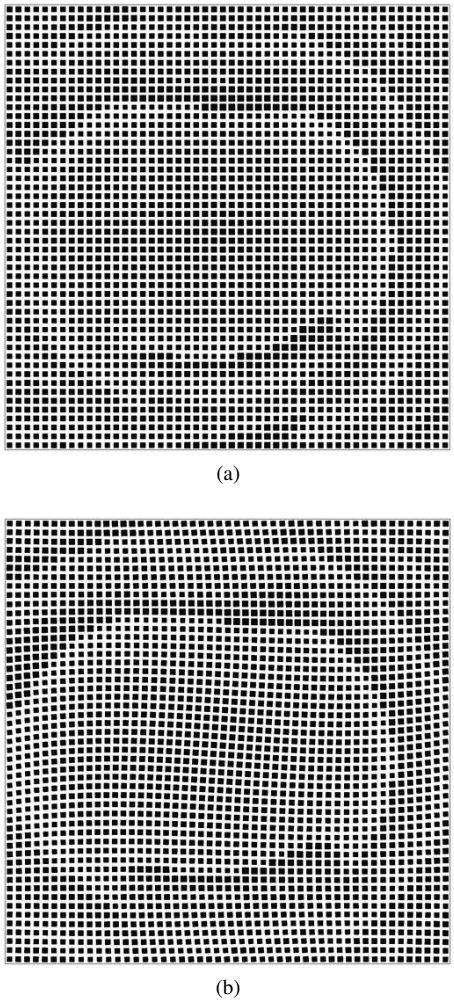

(a)

(b)

Figure 5. Reflectarray layout of (a) sample I and (b) sample II.

polarizations, V and H, at $10\,\mathrm{GHz}$. The reflectarray in Figure 5b, sample II, is optimized with the same optimization goals as for sample I, but only V-polarization and also at $10\,\mathrm{GHz}$. However, the sample is an irregular design where the array elements are positioned in an irregular grid. For this design, 10 distortion coefficients are included in the optimization.

For both samples, a corrugated horn with a taper of $-17.5\,\mathrm{dB}$ at 30° at $10\,\mathrm{GHz}$ is used as feed. The feed has been measured at the DTU-ESA-Spherical Near-Field Test Facility, and its measured pattern is used in the optimization.

The reflectarrays samples were measured for both V- and H-polarizations at a series of frequencies from $9.6\,\mathrm{GHz}$ to $10.5\,\mathrm{GHz}$. For the peak directivity, the measurements have a 1σ uncertainty of $0.05\,\mathrm{dB}$.

3.2. Simulations Versus Measurements

In Figure 6 and Figure 7, the radiation patterns of sample I and II for V-polarization at $10\,\mathrm{GHz}$ are shown. It is seen that both antennas radiate a high-gain beam on the European coverage. For sample I, which is optimized for dual-polarization, a minimum co-polar directivity of $26.5\,\mathrm{dBi}$ is obtained, whereas sample II, which is optimized for a single polarization, has a minimum directivity of $27.3\,\mathrm{dBi}$. The measured cross-polar radiation has been successfully suppressed below $0\,\mathrm{dBi}$ for both samples. It is also seen for sample II in Figure 7b that the co-polar radiation on the southern African coverage has been suppressed below $3\,\mathrm{dBi}$. This is however not the case for sample I where the co-polar radiation within the southern African coverage is higher than expected. During the design of sample I, the expected isolation level was above $25\,\mathrm{dB}$, but the measurements showed an isolation level around $17\,\mathrm{dB}$. The source of error was found to be an inadequate number of basis functions used in the SDMoM to characterize the electric currents on the patches during the design process. The analysis was not entirely converged in the entire forward hemisphere and resulted in a non-optimum design. By increasing the number of basis functions, we obtain the results shown in Figure 6.

A comparison of the solid and dotted lines, in Figure 6 and 7, shows an excellent agreement between simulations and measurements, where the high gain curves practically coincide. Also the accuracy for the lower levels is very

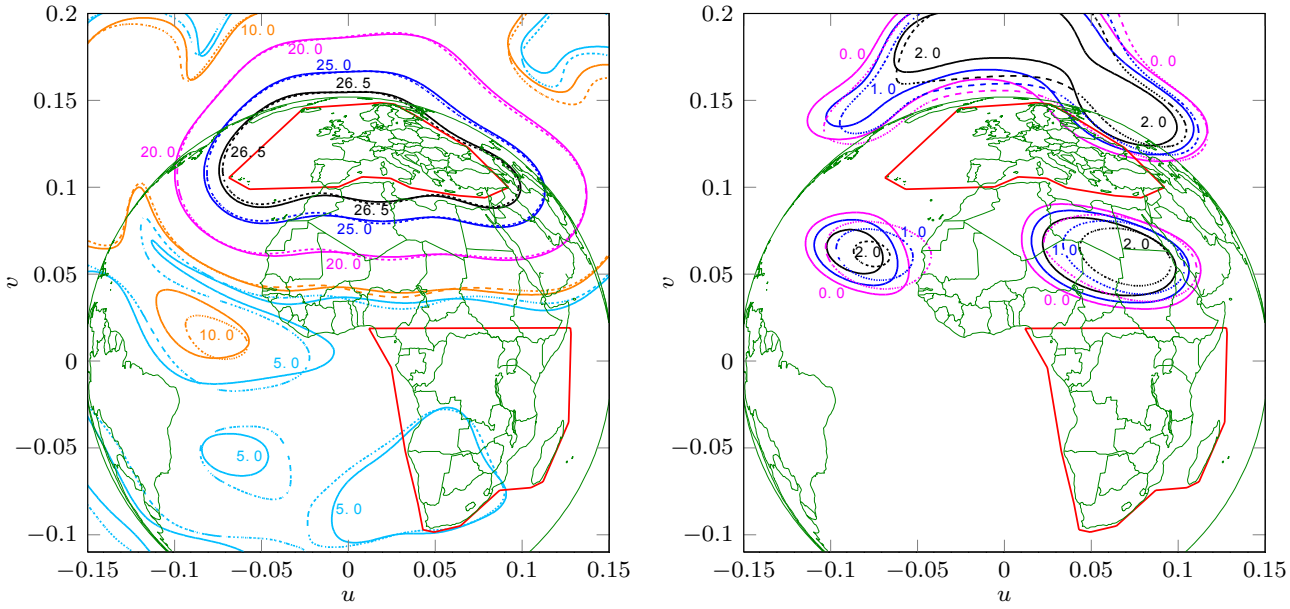

(a) (b)

Figure 6. Simulated (solid) and measured (dotted) radiation patterns of sample I for V-polarization at 10 GHz*, (a) co-polar pattern and (b) cross-polar pattern.*

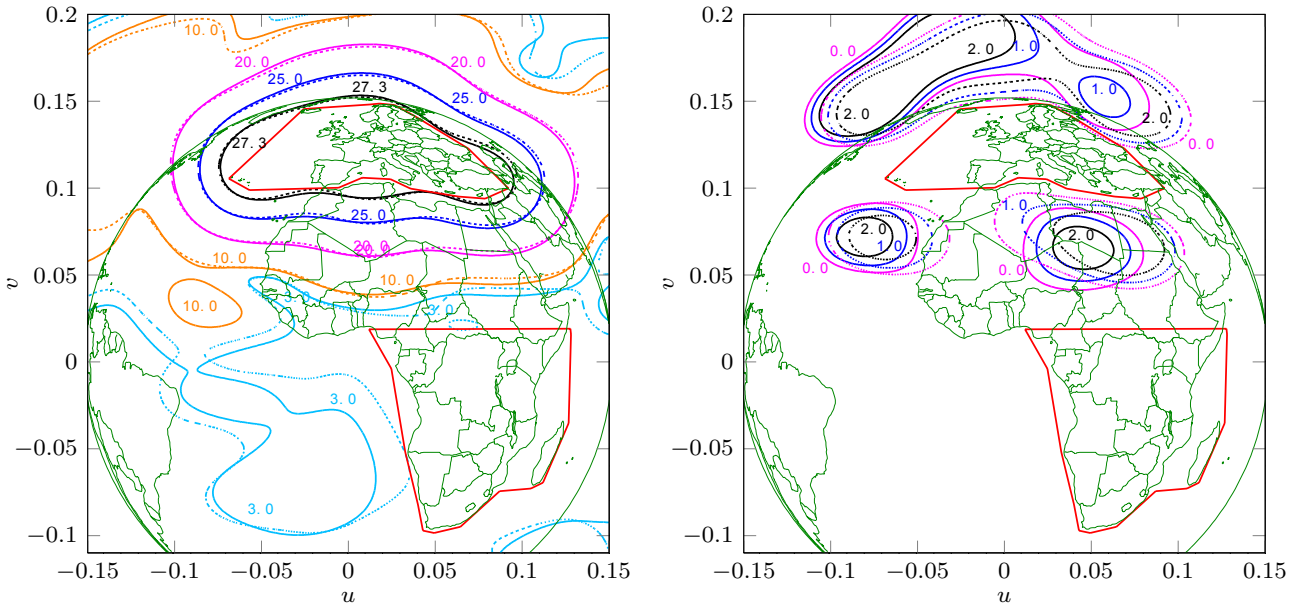

(a) (b)

Figure 7. Simulated (solid) and measured (dotted) radiation patterns of sample II for V-polarization at 10 GHz*, (a) co-polar pattern and (b) cross-polar pattern.*

good. This is the case for both samples I and II. The performance of the samples are summarized in Table 2. It is seen that the peak and minimum directivity within the European coverage are perfectly predicted for both samples in both polarizations. Even for the XPD and the isolations level, which are approximately 30 dB below the co-polar peak, the accuracy is good. The accuracy for the other measured frequencies is also very good; in all cases the maximum difference in the minimum co-polar directivity is 0.1 dB.

These excellent agreements between simulations and measurements for the presented reflectarrays are similar

Table 2. Measured Versus Simulated Data at $10\,\mathrm{GHz}$

Sample I	Peak directivity (dBi)	Min. directivity (dBi)	Min. XPD (dB)	Min. isolation (dB)
Meas. (V)	28.3	26.5	27.1	17.5
Sim. (V)	28.2	26.6	25.0	17.8
Meas. (H)	27.9	26.5	27.7	18.4
Sim. (H)	27.9	26.5	25.5	17.2
Sample II	Peak directivity (dBi)	Min. directivity (dBi)	Min. XPD (dB)	Min. isolation (dB)
Meas. (V)	29.2	27.3	27.2	24.3
Sim. (V)	29.2	27.3	27.8	27.2
Meas. (H)	29.4	27.1	24.5	20.2
Sim. (H)	29.4	27.1	21.0	20.5

to those obtained for conventional shaped reflector antennas, and clearly demonstrates the accuracy of the proposed DOT.

4. DESIGN OF LARGE CONTOURED BEAM REFLECTARRAY

To demonstrate the DOT's ability to design electrically large reflectarrays, an offset $1.5 \times 1.5\,\mathrm{m}^2$ contoured beam reflectarray that radiate a high-gain beam on the European coverage in the frequency range $9.5 - 10.5\,\mathrm{GHz}$ is designed. At the center frequency $10\,\mathrm{GHz}$, the dimension of the reflectarray corresponds to $50 \times 50\,\lambda_0^2$, with λ_0 being the free-space wavelength. It is optimized for both V- and H-polarizations including cross-polar suppressions within the European coverage. A linearly polarized Gaussian beam with a taper of $-25\,\mathrm{dB}$ at 30° is used as feed and square patches positioned in a regular grid are used as array elements. A scattering matrix look-up table for frequencies $f = 9.5,\ 10,\ 10.5\,\mathrm{GHz}$ has been calculated. The geometrical parameters are summarized in Table 3.

Initially, a reflectarray optimized using 50×50 splines is designed. A minimum co-polar directivity of $27.5\,\mathrm{dBi}$ within the European coverage is achieved in the specified frequency range for both polarizations. This design is subsequently used as the starting point for the final design where all patches are directly optimized. The final layout of the reflectarray is shown in Figure 8 and the performance summarized in Table 4. It is seen that the minimum directivity is above $28.3\,\mathrm{dBi}$ in the $9.5 - 10.5\,\mathrm{GHz}$ frequency range for both polarizations, and that the minimum XPD is around $27.0\,\mathrm{dB}$. It is expected that the XPD levels can be improved if a reduction in the minimum directivity is allowed. At $9\,\mathrm{GHz}$ and $11\,\mathrm{GHz}$, which are outside of the specified frequency range, the minimum directivity drops several dBs, thus demonstrating that the reflectarray has been successfully optimized to operate in the specified frequency range. Compared to the two previous reflectarray samples, the minimum directivity is improved by less than $2\,\mathrm{dB}$, even though the antenna area is more than 4 times larger. This is expected as this design is a multi-frequency design, and that the minimum directivity for contoured beam antenna scales differently with respect to the antenna size than pencil beam antennas [26].

Table 3. Reflectarray Data

Frequency	$9.5 - 10.5\,\mathrm{GHz}$
Reflectarray dimension	$1.5\,\mathrm{m} \times 1.5\,\mathrm{m}$
Number of elements	110×110
Relative permittivity	$\epsilon_\mathrm{r} = 3.66$
Loss tangent	$\tan\delta = 0.0037$
Substrate thickness	$h = 1.524\,\mathrm{mm}$
Feed distance	$d_\mathrm{f} = 1.5\,\mathrm{m}$
Feed offset angle	$\theta^\mathrm{i} = 30^\circ,\ \phi^\mathrm{i} = 0^\circ$
Main coverage	European coverage
Cross-polar suppression	European coverage

Due to the large electrical size of the reflectarray, the far-field requirements are specified in many far-field stations within the coverage [27]. With the cross-polar suppression, dual polarization, and three frequencies included in the optimization, the total number of far-field samples in the optimization is approximately 8200. This, together with 110×110 optimization variables, is rather demanding, resulting in an overall optimization time slightly below 20 hours using an $1.86\,\mathrm{GHz}$ 8 core Intel Xeon processor computer. Compared to POS for the design of shaped reflectors, the overall computation time is still high, and techniques to reduce this is currently being investigated.

Although square patches are used in this design, a 10% bandwidth is still achieved. However, it is expected that an improved performance can be obtained by using more advanced array elements e.g. rectangular patches or those reported in [6].

5. CONCLUSION AND ON-GOING WORK

An accurate and efficient direct optimization technique (DOT) for the design of contoured beam reflectarrays is presented. It is based on the Spectral Domain Method of Moments, Local Periodicity approach, and a minimax optimization algorithm. Contrary to the conventional phase-only optimization techniques, the geometrical parameters of the array elements are directly optimized to fulfill the contoured beam requirements. To ensure an accurate and efficient optimization procedure, higher-order hierarchical Legendre basis functions are used together with a fast yet accurate far-field calculation technique. The DOT can be used to design reflectarrays based on a regular grid as well as an irregular grid. Both co- and cross-polar radiation can be optimized for multiple frequencies, polarizations, and feed illuminations.

To show the accuracy of the DOT, two offset contoured beam reflectarrays that radiate a high-gain beam on an

Table 4. Performance of $50 \times 50\,\lambda_0^2$ *Reflectarray Design*

	V-polarization		H-polarization	
Frequency (GHZ)	Minimum Directivity (dBi)	Minimum XPD (dB)	Minimum Directivity(dBi)	Minimum XPD (dB)
9.0	23.4	25.2	22.8	18.8
9.5	28.7	27.0	28.4	26.7
10.0	28.7	27.8	28.3	28.0
10.5	28.5	28.0	28.3	27.5
11.0	23.5	23.1	25.0	27.1

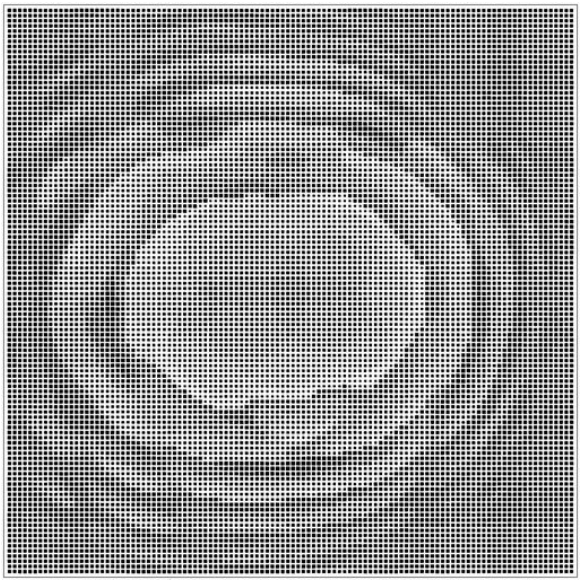

Figure 8. Reflectarray layout of $50 \times 50\,\lambda_0^2$ *design.*

European coverage have been designed, manufactured, and measured at the DTU-ESA Spherical Near-Field Antenna Test Facility. Excellent agreements are obtained for the simulated and measured patterns, showing accuracies that are comparable to those obtained for shaped reflectors. To demonstrate the DOT's ability to optimize electrically large reflectarrays, a 50×50 square wavelengths dual polarized contoured beam reflectarrays has been designed.

Several further developments of the DOT are on-going and worth mentioning. First, the orientation of the array elements can be added as optimization variables and exploited as extra degrees of freedom with the aim of improving the performance. This can also be used for the design of circularly polarized reflectarrays. Second, only square patches on a single layer substrate with rectangular rim are presented in this work. The DOT is applicable for more advanced and broadband elements, but will also allow multi-layer configurations with circular or elliptical rim. Finally, techniques for reducing the overall optimization time are currently being investigated.

ACKNOWLEDGMENTS

This work is supported by the European Space Agency (ESA) within the ESTEC contract No.4000101041, and Dr. S. Pivnenko, Technical University of Denmark, is acknowledged for the accurate measurements of the reflectarray samples.

REFERENCES

[1] J. A. Encinar, "Recent advances in reflectarray antennas," in *Proc. EuCAP*, Barcelona, Spain, 2010.

[2] H. Legay, D. Bresciani, E. Girard, R. Chiniard, E. Labiole, O. Vendier, and G. Caille, "Recent developments on reflectarray antennas at Thales Alenia Space," in *Proc. EuCAP*, Berlin, Germany, 2009.

[3] A. Roederer, "Reflectarray antennas," in *Proc. EuCAP*, Berlin, Germany, 2009.

[4] D. M. Pozar, S. D. Targonski, and H. D. Syrigos, "Design of millimeter wave microstrip reflectarrays," *IEEE Trans. Antennas Propag.*, vol. 45, no. 2, pp. 287–296, 1997.

[5] M. E. Bialkowski and K. H. Sayidmarie, "Investigations into phase characteristics of a single-layer reflectarray employing patch or ring elements of variable size," *IEEE Trans. Antennas Propag.*, vol. 56, no. 11, pp. 3366–3372, 2008.

[6] L. Moustafa, R. Gillard, F. Peris, R. Loison, H. Legay, and E. Girard, "The phoenix cell: a new reflectarray cell with large bandwidth and rebirth capabilities," *IEEE Antennas Wireless Propag. Lett.*, vol. 10, pp. 71–74, 2011.

[7] M. Bozzi, S. Germani, and L. Perregrini, "Performance comparison of different element shapes used in printed reflectarrays," *IEEE Antennas Wireless Propag. Lett.*, vol. 2, no. 1, pp. 219–222, 2003.

[8] J. Huang and R. J. Pogorzelski, "A Ka-band microstrip reflectarray with elements having variable rotation angles," *IEEE Trans. Antennas Propag.*, vol. 46, no. 5, pp. 650–656, 1998.

[9] D. Kurup, M. Himdi, and A. Rydberg, "Design of an unequally spaced reflectarray," *IEEE Antennas Wireless Propag. Lett.*, vol. 2, pp. 33–35, 2003.

[10] A. Capozzoli, C. Curcio, E. Iavazzo, A. Liseno, M. Migliorelli, and G. Toso, "Phase-only synthesis of a-periodic reflectarrays," in *Proc. EuCAP*, Rome, Italy, 2011, pp. 987 – 991.

[11] J. A. Encinar, M. Arrebola, and G. Toso, "A parabolic reflectarray for a bandwidth improved contoured beam coverage," in *Proc. EuCAP*, Edinburgh, UK, 2007.

[12] J. A. Encinar and J. A. Zornoza, "Three-layer printed reflectarrays for contoured beam space applications," *IEEE Trans. Antennas Propag.*, vol. 52, no. 5, pp. 1138–1148, 2004.

[13] J. A. Encinar, L. S. Datashvili, J. A. Zornoza, M. Arrebola, M. Sierra-Castaner, J. L. Besada-Sanmartin, H. Baier, and H. Legay, "Dual-polarization dual-coverage reflectarray for space applications," *IEEE Trans. Antennas Propag.*, vol. 54, no. 10, pp. 2827–2837, 2006.

[14] H. Legay, D. Bresciani, E. Labiole, R. Chiniard, E. Girard, G. Caille, L. Marnat, D. Calas, R. Gillard, and G. Toso, "A 1.3 m earth deck reflectarray for a Ku band contoured beam antenna," in *Proc. 33rd ESA Antenna Workshop*, Noordwijk, The Netherlands, 2011.

[15] J. A. Encinar, M. Arrebola, L. D. L. Fuente, and G. Toso, "A transmit-receive reflectarray antenna for direct broadcast satellite applications," *IEEE Trans. Antennas Propag.*, vol. 59, no. 9, pp. 3255–3264, 2011.

[16] O. M. Bucci, A. Capozzoli, G. D'Elia, P. Maietta, and S. Russo, "An advanced reflectarray design technique," in *Proc. 28th ESA Antenna Workshop*, Noordwijk, The Netherlands, 2005.

[17] A. Capozzoli, C. Curcio, A. Liseno, M. Migliorelli, and G. Toso, "Power pattern synthesis of advanced flat aperiodic reflectarrays," in *Proc. 33th ESA Antenna Workshop*, Noordwijk, The Netherlands, 2011.

[18] "DTU-ESA Spherical Near-Field Antenna Test Facility," *http://www.dtu.dk/centre/ems/English/research/facilities.aspx*.

[19] M. Zhou, S. B. Sørensen, P. Meincke, E. Jørgensen, O. S. Kim, O. Breinbjerg, and G. Toso, "Design and analysis of printed reflectarrays with irregularly positioned array elements," in *Proc. EuCAP*, Prague, Czech Republic, 2012.

[20] ——, "Design of dual-polarized contoured beam reflectarrays with cross-polar and sidelobe suppressions," in *Proc. IEEE AP-S Int. Symp.*, Chicago, Illinois, USA, 2012.

[21] M. Zhou, S. B. Sørensen, E. Jørgensen, P. Meincke, O. S. Kim, and O. Breinbjerg, "An accurate technique for calculation of radiation from printed reflectarrays," *IEEE Antennas Wireless Propag. Lett.*, vol. 10, pp. 1081–1084, 2011.

[22] E. Jørgensen, J. Volakis, P. Meincke, and O. Breinbjerg, "Higher order hierarchical Legendre basis functions for electromagnetic modeling," *IEEE Trans. Antennas Propag.*, vol. 52, no. 11, pp. 2985 – 2995, 2004.

[23] M. Zhou, E. Jørgensen, O. S. Kim, S. B. Sørensen, P. Meincke, and O. Breinbjerg, "Accurate and efficient analysis of printed reflectarrays with arbitrary elements using higher-order hierarchical Legendre basis functions," *IEEE Antennas Wireless Propag. Lett.*, vol. 11, pp. 814–817, 2012.

[24] M. Zhou, S. B. Sørensen, E. Jørgensen, P. Meincke, O. S. Kim, and O. Breinbjerg, "Direct optimization of printed reflectarrays for contoured beam satellite antennas applications," *Submitted to IEEE Trans. Antennas Propag.*, 2012.

[25] M. Zhou, S. B. Sørensen, E. Jørgensen, P. Meincke, O. S. Kim, O. Breinbjerg, and G. Toso, "Generalized direct optimization technique for printed reflectarrays," *In writing*, 2012.

[26] S. B. Sørensen, R. Jørgensen, and K. Pontoppidan, "Synthesis of the aperture field for a contoured beam," in *Proc. 7th ICAP*, York, United Kingdom, 1991.

[27] *POS, User's Manual*. TICRA Engineering Consultants, 2011.